

Size effect in concrete blocks under local pressure

R. Ince†

Firat University, Engineering Faculty, Civil Engineering Department, Elazig, Turkey

E. Arici‡

Firat University, Technical Education Faculty, Construction Education Department, Elazig, Turkey

(Received July 13, 2004, Accepted December 3, 2004)

Abstract. Numerous tests on concrete structure members under local pressure demonstrated that the compressive strength of concrete at the loaded surface is increased by the confinement effect provided by the enveloping concrete. Even though most design codes propose specific criteria for preventing bearing failure, they do not take into consideration size effect which is an important phenomenon in the fracture mechanics of concrete/reinforced concrete. In this paper, six series of square prism concrete blocks with three different depths (size range = 1:4) and two different height/depth ratios of 2 and 3 are tested under concentrated load. Ultimate loads obtained from the test results are analysed by means of the modified size effect law (MSEL). Then, a prediction formula, which considers effect of both depth and height on size effect, is proposed. The developed formula is compared with experimental data existing in the literature. It is concluded that the observed size effect is in good agreement with the MSEL.

Key words: concrete; bearing strength; size effect law; modified size effect law.

1. Introduction

Concrete bearing strength determination is necessary for the design of concrete/reinforced concrete members such as steel base plates of stanchions over concrete footings, building columns on concrete pedestals, bridge bearing on concrete piers, anchorages in post-tensioned concrete beams, concrete hinges and foundations of hydraulic structures. Most design codes (ACI-318 2002, EC2 1992, EC3 1992, TS500 1984) have used the square-root formula by Hawkins (1968), which does not account for size effect, for determining bearing capacity of concrete. However, it is well known that strength of concrete structures generally tends to decrease with increasing structure size. Size effect in concrete/reinforced concrete structures can be well explained by fracture mechanics.

The experimental investigations on fracture mechanics of cementitious materials until 1970s indicated that classical linear elastic fracture mechanics (LEFM) is invalid for quasi-brittle materials such as concrete. This inapplicability of LEFM is due to existence of an inelastic zone with large scale and full cracks in front of the main crack tip in concrete. This so-called fracture process zone

† Ph.D., Corresponding author, E-mail: rince@firat.edu.tr

‡ Ph.D.

(FPZ) is ignored by LEFM. Consequently, several investigators have developed non-linear fracture mechanics approaches to describe failure of concrete structures. Deterministic size effect laws among these non-linear approaches, for instance Size Effect Law (SEL) by Bazant (1984) and Modified Size Effect Law by Kim and Eo (1990), suggest that size effect on strength is primarily related to a relatively large FPZ in concrete. One of the main requirements in these laws is the need to test samples, which are geometrically similar and made of the same material, and which must provide a minimum size range = 1:4. In practice, the effect of specimen size on strength of concrete has been investigated by means of SEL for specimens of Modes I-III (Bazant and Pfeiffer 1987, Bazant and Şener 1987, Bazant and Prat 1988), while various attempts to apply MSEL to the compression-loaded specimens have been reported in the literature (Kim and Eo 1990, Kim *et al.* 1999, 2000, 2001).

The size effect in bearing strength of concrete was first investigated by Niyogi (1974) for cube specimens, experimentally. Ahmed *et al.* (1998) studied size effect on the square concrete blocks with height/depth ratio of 1.5 and loaded over a limited area, both theoretically and experimentally. Nevertheless, size range of specimens used in the above two investigations is not accurate for applying the deterministic size effect approaches. Ince and Arici (2004) first presented a deterministic approach derived from the experimental results on size effect in bearing strength of concrete cube specimens with size range=1:4.

In this study, six series of geometrically similar concrete square prism specimens of different size (size range 1:4) are tested by concentric bearing loading. The maximum loads obtained from the test results are analysed by using MSEL, and an approximate formula based on MSEL predicting bearing strength of concrete is developed. Such a formula indicates a good agreement with 34 existing test data in the literature (Hawkins 1968, Niyogi 1973, Ahmed *et al.* 1998).

2. Bearing strength of concrete

Experiments on concrete structural members under local pressure indicated that the compressive strength of concrete at the bearing area is increased by the confinement effect provided by the enveloping concrete. Failure of the member leads to a splitting crack directly under the localized load due to the transverse tensile stresses, as is shown in Fig. 1(a). Previous investigators found that bearing resistance of concrete is highly affected by the loaded area, cross-section of the loaded member, size of specimen, height of specimen, loading conditions and the compressive strength of concrete.

The bearing strength in construction materials was first investigated by Bauschinger (1876). For bearing strength, he proposed the well-known cube-root formula, which is based on a limited number of tests on sandstone cubes and, unfortunately, gives us incorrect results for concrete. Meyerhof (1953) and Shelson (1957) emphasized that failures of concrete subjected to concentrated loading are similar to those observed in triaxial compression test. To explain bearing failure in concrete block, Au and Baird (1960) developed a theory on the formation of an inverted pyramid under the loading plate. They assumed that the downward penetration of the inverted pyramid prior to failure would cause horizontal pressures. The resultant of these pressures was assumed to produce combined tension and bending in the concrete block. Failure would then occur when the maximum tensile stress at the top of the block exceeds the tensile strength of the concrete. Although this theory can be realistic for crack initiation, it does not seem reasonable at the final failure (Hawkins 1960).

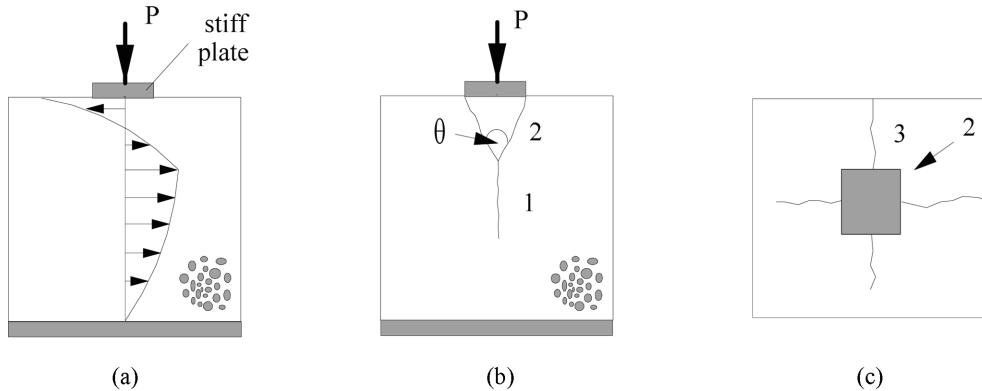


Fig. 1 Failure mechanism in bearing test (a) occurrence of bearing stress, (b) vertical cracking, (c) final failure

Hawkins (1968) proposed a realistic approach on the bearing strength of concrete by performing tests on concrete blocks supported on a stiff support and loaded through a rigid plate. He observed that, as the load is gradually increased, the first crack labelled 1 in Fig. 1(b) occurs in the vertical direction inside the block. When the maximum load is reached, a conical wedge labelled 2 in Fig. 1(b) punches out from beneath the bearing plate, and the radial cracks labelled 3 in Fig. 1(c) emerge on the loading surface. Typically, four radial cracks occur as indicated in Fig. 1(c). However, there also exist cases with more cracks. Moreover, experiments have revealed that the apex angle, θ , of the pyramid in Fig. 1(b) approximately varies from 38 to 70 deg (Hawkins 1960, Shelson 1957, Au and Baird 1960, Hawkins 1968).

Niyogi (1973, 1974) investigated the effect of some factors, such as specimen geometry, nature of support, eccentricity, mix properties, strength of concrete and specimen size, on the bearing resistance of concrete. Ahmed *et al.* (1998) performed experiments on square concrete blocks with a height/depth ratio of 1.5 and two different depth values (200, 400 mm). It was concluded that the ratio of bearing capacity of large to small concrete blocks can approximately be scaled to $1/S^{1/4}$, where S is the scale factor. Ince and Arici (2004) tested 54 cube specimens with size range = 1:4 under concentrated load, and proposed an approximate formula, based on the extended size effect law (Bazant 2002), for estimating bearing strength of concrete cubes.

In practice, two solutions are used to prevent failure of bearing in concrete/reinforced concrete/pre-stressed concrete structures. These are: (1) placing reinforcement in the tension zone; (2) limiting the bearing stresses in order to prevent the internal cracking (MacGregor 1992). However, the existing design codes generally prefer the second approach. This provides the following square-root formula by Hawkins:

$$q = \frac{P_u}{A_1} = f'_c \sqrt{R}, \quad R = \frac{A_c}{A_1} \quad (1)$$

where q , P_u and f'_c refer to the bearing strength, the failure load and the compressive strength of concrete, respectively. A_1 is the bearing area and A_c is called the effective area. It is assumed that load P spreads out into the concrete block at a slope of 2 horizontal to 1 vertical to the level at which spreading first reaches the edge of the block. The area A_c is calculated at this level, as is clearly described in Fig. 2.

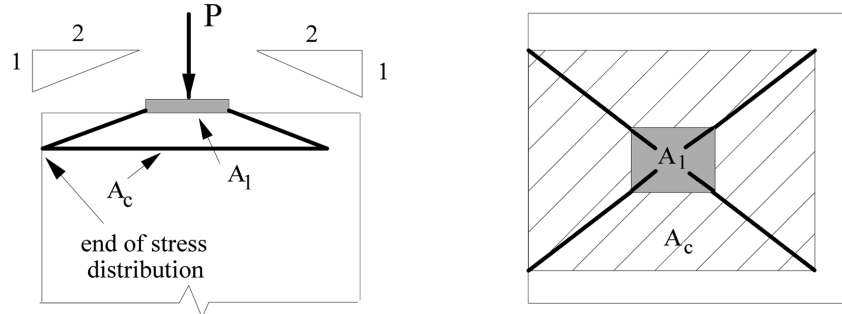


Fig. 2 Definition of A_1 and A_c areas

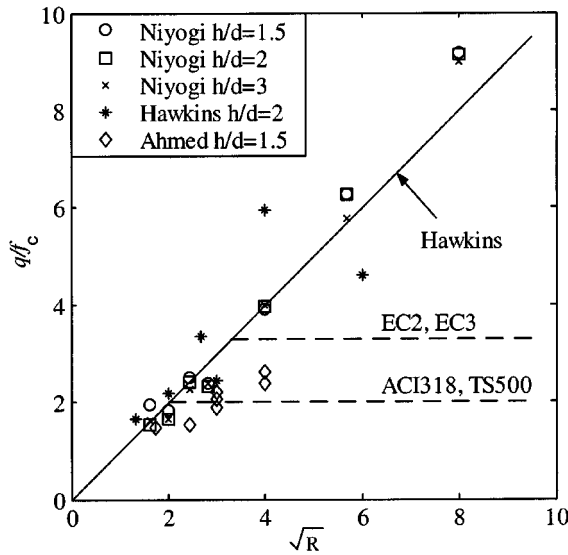


Fig. 3 Comparison of Hawkins and design codes approaches with existing test data

ACI-318 (2002) and TS500 (1984) limit the bearing strength of concrete according to $q \leq 2f'_c$, while the bearing capacity of concrete is restricted to 3.3 times of the compressive strength of concrete by EC2 (1992) and EC3 (1992). Nevertheless, these bounds are often on the side of extreme safety for high R ratios, as is shown in Fig. 3. In this figure, test results of some investigators (only specimens with the ratio of height/depth >1 are considered in this study), Eq. (1) and the lower bound of design codes are illustrated, comparatively in the q/f'_c against \sqrt{R} diagram. The geometric and material properties and loading conditions for the test specimens in Fig. 3 are reported in Table 1. Note that the cubic strength f_c [MPa] values have been converted to the cylindrical strength f'_c in Table 1, according to the following expression by Neville (1995):

$$f'_c = \left[0.76 + 0.2 \log \left(\frac{f_c}{19.58} \right) \right] f_c \tag{2}$$

Table 1 The investigations on bearing strength of concrete blocks in the literature

Ref.	n	R	f'_c [MPa]	d_{\max} [mm]	d [mm]	h/d	Cross section	Loading plate	Loading case
Hawkins (1968)	6	1.8-36	11.3-33.5	1.5	101.6, 152.4	2	circular	circular	concentric
Niyogi (1973)	80	2.67-64	19.7-25.8*	12.7	203.2	1.5, 2, 3	square	square, rectangular	concentric
Ahmed <i>et al.</i> (1998)	9	3-16	50.3*	20	200, 400	1.5	square	square, rectangular	concentric, eccentric

n = number of specimens, d_{\max} = maximum aggregate size, d = specimen depth, h = specimen height.

*converted from cube strength to cylinder strength

3. Size effect in concrete fracture

Numerous experiments on geometrically similar concrete/reinforced concrete specimens of different sizes revealed that the nominal strength tends to decrease with increasing their sizes. This is called size effect in fracture mechanics of concrete/reinforced concrete. Size effect cannot be explained by classical continuum theories like elasticity and plasticity, which have been widely used by the existing design codes for concrete structures. As specimen size increases, the strength is expected to decrease due to the probability of presence of flaws.

Historically, the fact that the strength of brittle materials is affected by the presence of imperfections was first suggested by Griffith (1920). Due to his conclusion, it can be expected that the value of the ultimate strength will depend upon the size of specimens. Subsequently, Weibull (1939) proposed the weakest-link theory based on a statistical approach which predicts a decreasing in material strength with increasing specimen volume. The theory has been used for estimating safety factors of materials. In the early 1980s, it was realized that neither LFM nor Weibull's approach were adequate for predicting size effect in cementitious materials (Walsh 1972, Bazant 1991). For this reason, several investigators have developed deterministic size effect theories based on non-linear fracture mechanics.

Besides the statistical based size effect, the second size effect referred to as the fracture-type size effect in concrete fracture has been described by Bazant (1984). This is referred to as the size effect law (SEL). Bazant derived SEL, by considering the energy balance at crack propagation, and dimensional analysis of geometrically similar specimens.

The so-called SEL is expressed as

$$\sigma_N = B\sigma_0 \left[1 + \frac{d}{d_0} \right]^{-1/2} \quad (3)$$

in which σ_N presents the nominal strength at failure. Such a strength is expressed as $\sigma_N = c_n P_u / td$, where d is characteristic dimension of the specimen, chosen to coincide with the specimen depth, t is the specimen thickness, and c_n is a constant depending on the load type. σ_0 is referred to as the strength parameter and B and d_0 are empirical constants which can be determined by curve fitting to the test results of geometrically similar specimens. This is an approach which expresses the size effect in concrete specimens based on fracture mechanics. SEL has been derived based on the

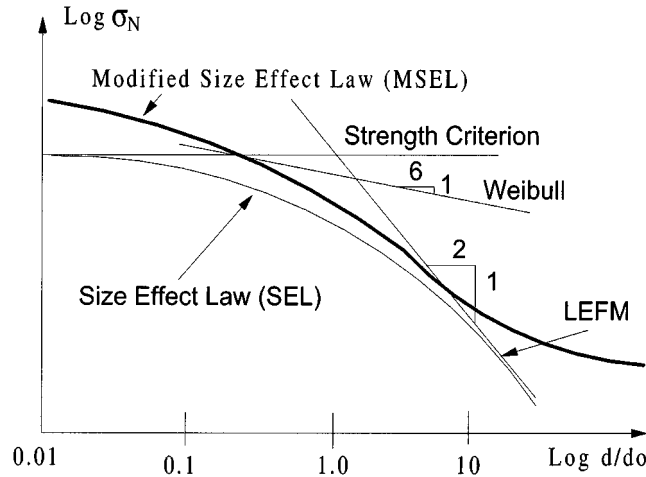


Fig. 4 Size Effect Law (SEL) and Modified Size Effect Law (MSEL)

following assumptions: the potential energy released during the fracture is proportional to the crack length (a), to the area of the cracking zone; the width of the front of cracking zone (nd_{\max}) is constant, where n is an empirical constant and d_{\max} is the maximum aggregate size.

SEL of Bazant is illustrated in Fig. 4. For small test specimens there is no size effect due to the strength at failure being proportional to the material strength. This case corresponds to the strength criterion, and is represented by the horizontal line in Fig. 4. In the large test specimens, we have the maximum possible size effect. The material strength at failure is proportional to a characteristic dimension and corresponds to the classical linear elastic fracture mechanics, which is represented by the inclined line with slope $-1/2$ in Fig. 4. The intersection of the two asymptotes corresponds to $d = d_0$ and is called the transitional size. The results of most concrete test specimens in existing experimental studies lie in the transition zone between these extreme cases. Contrary to LEFM, size effect in the Weibull-type statistical approach is characterized a straight line with slope $-1/6$, as is shown in Fig. 4 (Bazant and Yavari 2005).

Size effect in concrete behaviour has been extensively studied both experimentally and theoretically with success (Bazant and Pfeiffer 1987, Bazant and Şener 1987, Bazant and Prat 1988, Marti 1989). However, some published experiments indicate results different from those predicted by the Bazant's SEL. Large concrete members without initial cracks such as Hasegawa's (1985) split-cylinder test specimens and Shioya's (1989) test beams can resist some stress. Consequently, Kim and Eo (1990) developed a modified size effect law (MSEL) based on the concept of dissimilar cracks, where an empirical constant of size independent strength σ_R is added to Eq. (3):

$$\sigma_N = B\sigma_0 \left[1 + \frac{d}{d_0} \right]^{-1/2} + \sigma_R \quad (4)$$

Eq. (4) is also called the extended size effect law in a different approach by Bazant (2002). According to MSEL, the size effect becomes insignificant for both very small and very large characteristic dimensions, as represented by the curved thick solid line in Fig. 4. In practice, d_0 in Eq. (4) is chosen about $2-3d_{\max}$ (Kim *et al.* 1999, 2000, 2001).

4. Experimental program

The test specimens considered are square prisms with the height-to-depth ratio equal to 2 and 3. To determine size effect, geometrically similar specimens with cross-sectional depths $d = 50, 100$ and 200 mm were tested. Not only size of specimen but also variables of the ratio of height/depth h/d , maximum aggregate size d_{\max} and ratio of effective area to the bearing area R are here considered in order to find a general expression of the bearing resistance strength of concrete. Six series specimens (54 prism specimens), namely A, B, C, D, E and F were tested concerning these three variables in different combinations. All specimens in each series were cast from the same batch of concrete. Three identical cylinder specimens with diameter 150 mm and length 300 mm were also cast from each batch of concrete to determine compressive strength of concrete. The maximum aggregate size was 4 mm for batch A, B, 8 mm for C, D and 16 mm for E, F, respectively. The maximum sand grain size was 4 mm for each batch. Mineralogically, the aggregate consisted of river sand. The aggregate and sand were air-dried prior to mixing. The Portland cement was used for the production of concrete mixtures which had a 28 day compressive strength of 32.5 MPa. The specimens were cast with the side of depth in a vertical position. All the specimens and cylinders were removed from the mold after 1 day and were subsequently cured till testing at 28 days, in a moist room of 95 percent relative humidity and temperature of about 25°C.

All the specimens were tested in a digital compression machine with a capacity of 2500 kN except for the largest specimens in height ($h = 600$ mm), which were tested in MFL system compression and bending machine with a capacity of 5000 kN. The specimens were loaded monotonically until failure, through smooth steel bearing plates with various areas according to the selected R values. Care was taken to apply a constant loading rate. Typically, it took about 8 min (± 30 sec) to reach the maximum load for each specimen size. The smooth bearing plates of high tensile steel were 10 mm thick. The steel plates did not indicate any flexural or any other deformation after testing. The identical cylinders were tested at an age similar to that of the square prism specimens.

5. Analysis of test results

5.1 Test results

For each of the 54 specimens, Table 2 summarizes the characteristic dimension d (specimen depth), the compressive strength f'_c of concrete, the maximum aggregate size d_{\max} , the value of R , the height/depth ratio h/d , the square bearing plate size a , the observed failure load P_u and the nominal strength σ_N according to Eq. (1). In the same table, the mean normalized nominal strength values ($\bar{\sigma}_N/f'_c\sqrt{R}$) and the average apex angles θ values of the pyramid, which takes form below the bearing plate, are also given for each specimen size.

As Niyogi (1974) and Ince and Arici (2004) previously observed in their studies, basically there was no difference between the behaviour of specimens having different sizes under similar concentrated loading. They had the typical vertical cracking more or less along the center line of one or more side faces as described in section 2. In addition, it was seen that three or more cracks spread radially from the loaded surface.

Table 2 Experimental results

Series	f'_c [MPa]	d_{\max} [mm]	R	h/d	a [mm]	d [mm]	P_u [kN]			$\sigma_N = P_u/d^2$ [MPa]			$\frac{\bar{\sigma}_N}{f'_c \sqrt{R}}$	θ (deg)
							1	2	3	1	2	3		
A	20.3	4	6.25	2	20	50	23.2	22.9	23.9	58.00	57.25	59.75	1.149	40
					40	100	82.7	86.3	88.3	51.69	53.94	55.19	1.056	47
					80	200	265	262.3	272.9	41.41	40.98	42.64	0.821	51
B	22.5	4	6.25	3	20	50	23.1	24.2	24.1	57.75	60.50	60.25	1.057	40
					40	100	92.7	90.2	89.7	57.94	56.38	56.06	1.009	45
					80	200	290	283	305	45.31	44.22	47.66	0.813	51
C	32.7	8	6.25	2	20	50	36.5	35.9	36.3	91.25	89.75	90.75	1.109	40
					40	100	136.7	134.1	134.7	85.44	83.81	84.19	1.034	46
					80	200	420.6	415.4	417.1	65.72	64.91	65.17	0.799	48
D	32.7	8	16.0	2	12.5	50	21.8	22.1	21.9	139.52	141.44	140.16	1.074	44
					25	100	81.5	80.8	82.7	130.40	129.28	132.32	1.000	51
					50	200	297.1	283.5	290.1	118.84	113.40	116.04	0.888	53
E	25.2	16	6.25	2	20	50	28.7	28.9	29.6	71.75	72.25	74.00	1.153	48
					40	100	106.2	107.8	107.9	66.38	67.38	67.44	1.064	52
					80	200	365	373	359.1	57.03	58.28	56.11	0.907	57
F	27.4	16	6.25	3	20	50	29.6	29.7	29.6	74.00	74.25	74.00	1.082	46
					40	100	112.3	113.9	118	70.19	71.19	73.75	1.047	52
					80	200	367	367	395	57.34	57.34	61.72	0.858	53

5.2 Analysis of test data

To obtain a general equation that can predict the bearing strength of concrete prism specimens at failure, all of the series are used in the analysis. For this reason, the term of σ_0 in Eq. (3) or Eq. (4) is taken as $f'_c \sqrt{R}$, proposed by Hawkins, since each test series involves different R ratios and compressive strength values f'_c . However, the following factors must be considered when a size effect formula on bearing strength of concrete is proposed.

5.2.1 Effect of maximum aggregate size on size effect

Eq. (4) is valid only for geometrically similar structures of specimens made of concrete with same maximum aggregate size d_{\max} . Nevertheless, it is found in the previous study by Ince and Arici (2004) that the effect of maximum aggregate size on the bearing capacity of concrete can be negligible within the practical range of size. Correspondingly, Kim *et al.* (1999) analysed the size effect on compressive strength of concrete cylinders by using total of 678 test data in the literature, and concluded that the effect of maximum aggregate size on size effect can be ignored.

5.2.2 Effect of apex angle of pyramid and height/depth ratio of specimen on size effect

The apex angles θ of the pyramids could not be accurately measured since the sides of the pyramids were not perfectly symmetrical. Nevertheless, it was observed that θ values vary from approximately 40 to 57°. The observed range is in good agreement with the range in the literature

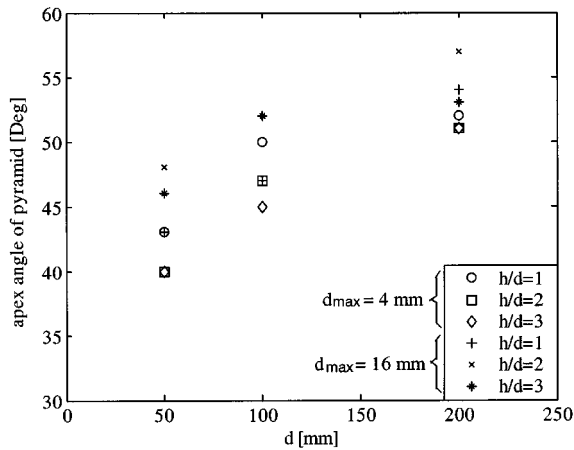


Fig. 5 Variation of apex angle of pyramid against specimen size, for different maximum aggregate sizes ($R = 6.25$)

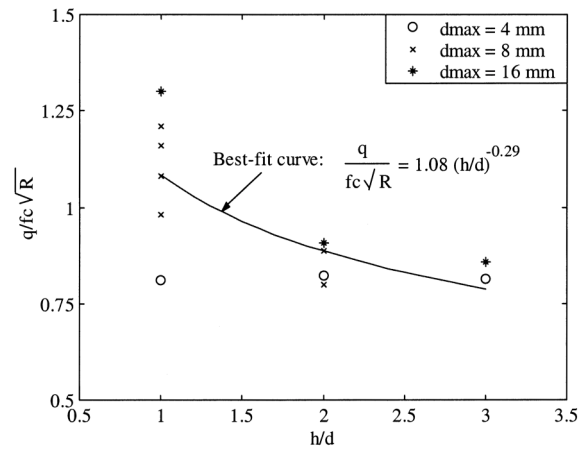


Fig. 6 Relation between specimen height/depth ratio and bearing strength, for different maximum aggregate sizes ($d = 200$ mm)

(Shelson 1957, Au and Baird 1960, Hawkins 1960, 1968). However, the average values of θ generally increase with increasing specimen depth, as is shown in Table 2. This means that this type of failure is similar to failure of Brazilian split-tension specimens. On the other hand, it is observed from Table 2 that the values of θ are not affected from the ratios of height/depth of samples. Furthermore, these values are approximately the same as the θ values measured on the cube specimens in the previous study by Ince and Arici (2004), in which cube sizes were $d = 50, 100$ and 200 mm. Fig. 5 shows, for different values of height/depth ratio (in which, $h/d = 1$ presents cube specimens (Ince and Arici 2004)), the apex angle of the pyramid against the specimen size, for two different maximum aggregate diameters.

Fig. 6 shows the mean values of the normalized bearing strength ($q/f_c \sqrt{R}$) against the variation of height/depth ratio (h/d), for the specimens with $d = 200$ mm in Table 2. In the same figure, the best-fit curve, expressed by a power function, is also given. As is shown in Fig. 6, the normalized strength significantly decreases for low h/d ratios while it slightly reduces for high h/d ratios. This type of decrease in strength is probably due to a reduced influence of the base friction force between the bearing plate and the sample with increasing the specimen height, and also due to size effect (Niyogi 1973). However, the large scatter at value of $h/d = 1$ shown in Fig. 6 is due to the high confinement effect under the bearing plate, because the confinement is inversely proportional to the specimen volume (Kim *et al.* 1999). Therefore, it may be concluded from Fig. 6 that, when investigating the effect of specimen size on bearing strength of concrete, it needs to make a distinction between cube ($h/d = 1$) and square prism block with $h/d > 1$.

5.2.3 Effect of failure mode of specimens on size effect

Failure in test of concrete blocks loaded over a limited area is due to axial splitting cracks, combined with frictional plasticity on the pyramid surface under the loading plate. In Table 2, if variation of the average apex angles of pyramid according to specimen size is considered, it is concluded that the height of pyramid decreases relatively as increasing specimen size. From this, the following two results can be noted: (1) for the small specimen size, the load to cause the splitting

crack is much higher than the load to cause frictional slip of the pyramid surface; (2) at large sizes, the ultimate load is reached by frictional plastic slip in a small highly confined pyramid under the bearing plate. This indicates that there is a transition to some non-brittle failure friction mechanism at the ultimate load for a certain sufficiently large size. Bazant proposes, for this type of failure, that it is necessary to add a lower limit value (σ_R) to size effect formula like MSEL. This might also be true for some other tests such as compression tests (Kim *et al.* 1999) and split-tension cylinder test (Bazant *et al.* 1991).

5.2.4 Derivation of the size effect relationship

From the above discussions, the nominal bearing strength of concrete blocks can be expressed by:

$$\sigma_N = f'_c \sqrt{R} \left\{ B \left[1 + \frac{d}{d_0} (h/d)^n \right]^{-1/2} + \alpha \right\} \tag{5}$$

in which B , d_0 , n and α are positive empirical constants. Eq. (5) takes into account the effects of both depth and height on size effect formula for the bearing strength of concrete blocks. A similar approach was also utilized for size effect on flexural compressive strength of concrete by Kim *et al.* (2001). In the present study, the Levenberg-Marquardt non-linear curve fitting algorithm was used for determining the empirical constants in Eq. (5):

$$\sigma_N = f'_c \sqrt{R} \left[\frac{1.03}{\sqrt{1 + \frac{d}{94.27} \left(\frac{h}{d}\right)^{0.22}}} + 0.32 \right] \text{ for } h/d > 1 \tag{6}$$

where f'_c is in MPa and d and h are in mm. Fig. 7 shows test data and Eq. (6) curve in the $\sigma_N/f'_c \sqrt{R}$ against $\sqrt{1 + d/94.27(h/d)^{0.22}}$ diagram. In the same figure, the statistical constants (correlation coefficient r and coefficient ω of variation (vertical deviations from the regression line)) for Eq. (6) are also given. The statistical constants indicate that Eq. (6) agrees with the test results quite well ($\omega < 0.100$, $r > 0.900$).

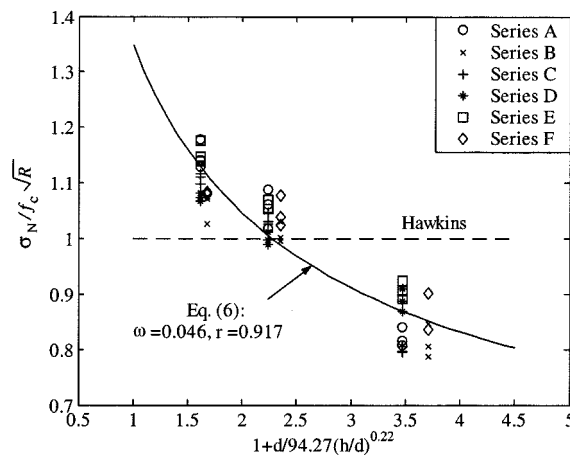


Fig. 7 Size effect in bearing test of concrete blocks

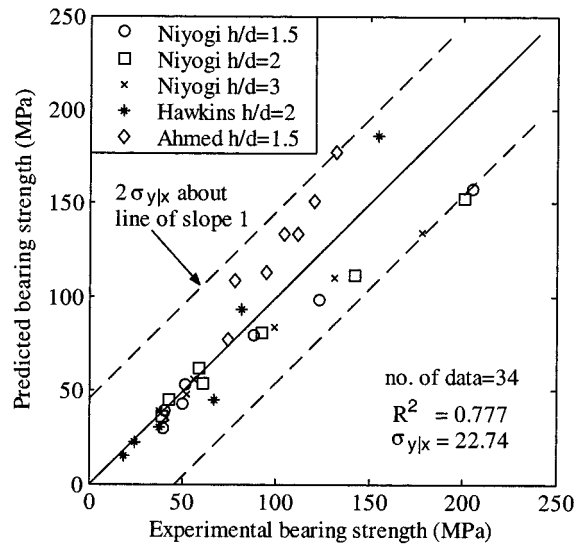


Fig. 8 Plots of experimental versus predicted values of concrete bearing strength

6. Comparison with previous studies

In previous investigations, some effects on the bearing strength of concrete blocks were evaluated (except for the work by Ahmed *et al.* 1998), as summarized in Table 1: R values, bearing plate shape, disposition of the bearing plate with respect to the center of loaded surface, and height/depth ratio. However, in the work of Ahmed *et al.*, size effect cannot be clearly revealed since size range is less than 1:4, and specimen sizes are $d = 200$ and 400 mm.

Fig. 8 shows the diagram of experimental versus predicted values of Eq. (6) for bearing capacity of concrete. The coefficient of determination R^2 , the standard error $\sigma_{x|y}$ and the approximate %5 and %95 confidence limits of the vertical deviations of the data points from the line of slope 1 between experimental and predicted bearing strength of concrete are also shown in Fig. 8. These confidence limits, marked in the Fig. 8, have been estimated on the basis of the Gaussian distribution by passing lines parallel to the line of slope 1 at vertical distances $\pm 2\sigma_{x|y}$. In spite of the large scatter, which is due to test data obtained from different laboratories for different concretes, the figure shows that Eq. (6) is in good agreement with the test results considered.

7. Conclusions

From the findings of these experimental and statistical investigations on size effect of bearing strength of square prism concrete blocks with the ratio of height/depth > 1 , the following conclusions can be drawn:

1. The present experimental data indicate that the nominal strength at failure decreases as the specimen size increases. Consequently, the present test results are in a good agreement with MSEL.

2. The nominal bearing strength significantly reduces for low height/depth ratios, while it decreases slightly for high height/depth ratios.
3. Although the height of pyramid beneath bearing plate decreases with the increasing size of specimen, it is independent of the specimen height/depth ratio.
4. From the comparison of previous test results with Eq. (6), such a relationship seems to be useful for determining bearing strength of square prism concrete blocks.

References

- ACI-318 (2002), *Building Code Requirements for Structural Concrete and Commentary*, Farmington Hills, Michigan.
- Ahmed, T.M.A., Burley, E. and Rigden, S. (1998), "Bearing capacity of plain and reinforced concrete loaded over a limited area", *ACI Struct. J.*, **95**(3), 330-342.
- Au, T. and Baird, D.L. (1960), "Bearing capacity of concrete blocks", *J. of the American Concrete Institute Proc.*, **56**(9), 869-879.
- Bauschinger, J. (1876), "Tests with blocks of natural stone", *Mechanisch und Technischen Laboratorium der Kgl.*, 6, p.13.
- Bazant, Z.P. and Yavari, A. (2005), "Is the cause of size effect on structural strength fractal or energetic-statistical?", *Engineering Fracture Mechanics*, **72**(1), 1-31.
- Bazant, Z.P. (1984), "Size effect in blunt fracture: concrete, rock and metal", *J. Eng. Mech.*, ASCE, **110**(4), 518-535.
- Bazant, Z.P. (1991), "Size effect on fracture and localization: apercu of recent advances and their extension to simultaneous fatigue and rate-sensitivity", *Proc. of the International RILEM/ESIS Conf.*, Noordwijk, June.
- Bazant, Z.P. (2002), *Scaling of Structural Strength*, Hermes-Penton, London.
- Bazant, Z.P. and Pfeffier, P.A. (1987), "Determination of fracture energy properties from size effect and brittleness number", *ACI Materials J.*, **84**(6), 463-480.
- Bazant, Z.P. and Prat, P.C. (1988), "Measurement of mode III fracture energy of concrete", *Nuclear Engineering and Design*, **106**, 1-8.
- Bazant, Z.P. and Şener, S. (1987), "Size effect in torsional failure of concrete beams", *J. Struct. Eng.*, ASCE, **113**(10), 2125-2136.
- Bazant, Z.P., Kazemi, M.T., Hasegawa, T. and Mazars, J. (1991), "Size effect in Brazilian split-cylinder tests: measurements and fracture analysis", *ACI Materials J.*, **88**(3), 325-332.
- EC2 (1992), *Design of Concrete Structures*, European Pre-Standard, Brussels.
- EC3 (1992), *Design of Steel Structures*, European Pre-Standard, Brussels.
- Griffith, A.A. (1920), "The phenomena of rupture and flow in solids", *Phil. Trans. Roy. Soc. London*, **A221**, 163-198.
- Hasegawa, T., Shioya, T. and Okada, T. (1985), "Size effect on splitting tensile strength of concrete", *Proc. of the JCI 7th Conf.*, Tokyo.
- Hawkins, N.M. (1960), "Discussion of work of Au and Baird (1960)", *J. of the American Concrete Institute Proc.*, **56**(9), 1469-1479.
- Hawkins, N.M. (1968), "The bearing strength of concrete loaded through rigid plates", *Magazine of Concrete Research*, **20**(62), 31-40.
- Ince, R. and Arici, E. (2004), "Size effect in bearing strength of concrete cubes", *Construction and Building Materials*, **18**(8), 603-609.
- Kim, J.K.K., Yi, S.T., Park, C.K. and Eo, S.H. (1999), "Size effect on compressive strength of plain and spirally reinforced concrete cylinders", *ACI Struct. J.*, **96**(1), 88-94.
- Kim, J.K.K. and Eo, S.H. (1990), "Size effect in concrete specimens with dissimilar initial cracks", *Magazine of Concrete Research*, **42**(153), 233-238.

- Kim, J.K.K., Yi, S.T. and Kim, J.H.J. (2001), "Effect of specimen sizes on flexural compressive strength of concrete", *ACI Struct. J.*, **98**(3), 416-424.
- Kim, J.K.K., Yi, S.T. and Yang, E.I. (2000), "Size effect on flexural compressive strength of concrete specimens", *ACI Struct. J.*, **97**(2), 291-296.
- MacGregor, J.G. (1992), *Reinforced concrete: Mechanics and Design*, Second Edition, Prentice-Hall, New Jersey.
- Marti, P. (1989), "Size effect in double-punch tests on concrete cylinders", *ACI Mater. J.*, **86**(6), 597-601.
- Meyerhof, G.G. (1953), "The bearing capacity of concrete and rock", *Magazine of Concrete Research*, **4**(12), 107-116.
- Neville, A.M. (1995), *Properties of Concrete*, Fourth Edition, Longman, London.
- Niyogi, S.K. (1973), "Bearing strength of concrete-geometric variation", *J. Struct. Div.*, ASCE, **99**(ST7), 1471-1490.
- Niyogi, S.K. (1974), "Concrete bearing strength-support, mix, size effect", *J. Struct. Div.*, ASCE, **100**(ST8), 1685-1701.
- Shelson, W. (1957), "Bearing capacity of concrete", *J. of the American Concrete Institute Proc.*, **54**(5), 405-414.
- Shioya, T. (1989), "Shear properties of large reinforced concrete member", Institute of Technology, Shimizu Corporation, Japan, Report No 25.
- TS-500 (1984), *Requirements for Design and Construction of Reinforced Concrete Structure*, Turkish Standard Institution, Ankara.
- Walsh, P.F. (1972), "Fracture of plain concrete", *Indian Concrete J.*, **46**(11), 469-470.
- Weibull, W. (1939), "A statistical theory of the strength materials", Swedish Royal Institute for Engineering Research, Stockholm.

Notation

a	: square bearing plate size (mm)
A_1	: bearing area (mm ²)
A_c	: effective area, as defined by ACI (mm ²)
B	: empirical constant
c_n	: constant depending on load type
d	: specimen depth (mm)
d_0	: empirical constant
d_{\max}	: maximum aggregate size (mm)
f_c	: concrete cube strength (MPa)
f'_c	: concrete cylinder strength (MPa)
h	: specimen height (mm)
n	: number of specimens, empirical constant
P_u	: ultimate load (kN)
q	: bearing strength (MPa)
R	: A_c/A_1
r	: correlation coefficient
R^2	: coefficient of determination
S	: scale factor
t	: specimen thickness (mm)
α	: empirical constant
θ	: apex angle of pyramid under bearing plate (deg)
σ_0	: strength parameter (MPa)
σ_N	: nominal strength (MPa)
σ_R	: size independent stress (MPa)
$\sigma_{x/y}$: standard error
ω	: coefficient of variation

FPZ : Fracture Process Zone
LEKM : Linear Elastic Fracture Mechanics
MSEL : Modified Size Effect Law
SEL : Size Effect Law